The Pennsylvania State University

The Graduate School

Department of Mechanical and Nuclear Engineering

EFFECTS OF SUPERCONDUCTOR ELECTRON SCREENING ON FUSION REACTION RATES

A Thesis in

Nuclear Engineering

by

Kamron C. Fazel

Submitted in Partial Fulfillment
of the Requirements
for the Degree of

Master of Science

May 2011

The thesis of Kamron Fazel was reviewed and approved* by the following:

Kostadin N. Ivanov
Distinguished Professor of Nuclear Engineering
Thesis Advisor

Qi Li
Professor of Physics

Thomas E. Mallouk
Professor of Chemistry
Professor of Physics

Arthur T. Motta
Professor of Nuclear Engineering and Materials Science and Engineering
Head of the Department of Mechanical and Nuclear Engineering

*Signatures are on file in the Graduate School

Abstract

This research explores fusion cross section enhancements from electron screening within superconductors and the feasibility of engineering a system to extract the energy from a superconductor fusion system. There have been claims that superconductors will exhibit "superscreening", which could largely increase fusion cross sections. However, there is currently no widely accepted theory to explain superconductor electron screening. With the possibility of significantly enhanced fusion cross sections in superconductors, this research analyzed the possibility of a net energy gain system.

To determine the contribution of electron screening from superconductor electron pairs, the first portion of this research proposes and analyzes an experiment. The proposed experiment would utilize the bombardment of deuterons (20 keV) on a PdD target in two separate stages, above and below the superconducting transition temperature (i.e., metallic and superconducting PdD states, respectively). The protons from the resulting fusion reactions would be detected to infer the electron screening differences between metallic and superconducting states of PdD. The pre-experimental analysis shows that the experiment would be able to determine the total screening from a superconductor with a 38% error of the screening energy with 95% confidence.

The second portion of the research investigated the possibility of net energy gain from fusion reactions within a superconductor. In order to do so, a simple direct energy conversion model was developed. The model accounted for energy losses due to fusion product energy deposition, energy conversion, and cooling requirements. With the model, a sample calculation of energy gain was performed on superconducting PdD. Using the Carnot efficiency of cooling and the PdD sample thickness equal to the coherence length (10^{-8} m), the calculation indicated that with the widely accepted 11 K transition temperature there would be no net energy gain. However, net energy gain may be possible if a superconductor were developed with a superconductor transition temperature above 100 K. Even if net energy gain was achievable, the reaction rates from lattice induced vibrations in superconducting PdD would result in an extremely low power density, thus rendering the device impractical.

Table of Contents

List of Figures

List of Tables

Acknowledgements

I thank my wife, Katherine, for keeping me focused and inspiring me to work hard. Thanks to Chris Hurd and his students, Mike Blanchard, Shelby Stoker, Fritz Koennecke, and Max Kellish for designing and building the test equipment that can be used for the proposed experiment. Thanks to Luke Allen for assisting the students. Thanks to Ryan Kinney for providing feedback to me as my thoughts developed. David J. Nagel edited and provided guidance in focusing my research. I also thank anyone willing to take risks on potentially significant ideas.

Chapter 1
Introduction

Tokamak and Inertial Confinement Fusion devices are complex and costly. Performance of these systems hinges on ensuring the plasma will be confined long enough at high enough temperatures and densities. The goal of this thesis is to consider the possibility of creating a fusion reactor that could function mostly in the solid state with direct energy conversion of the charged fusion products. However, this is not currently possible, because fusion cross sections are low, leading to lost energy in attempt to fuse nuclei. If there was a way to make fusion reactions more probable with a way to extract the energy, then a fusion energy system could be more practical. One possible method of increasing the probability of fusion events occurring would be to reduce the Coulomb barrier by means of electron screening. The concepts and determination of electron screening in materials are considered in this thesis. It is theororized that a superconductor may offer exceptional Coulomb barrier reduction. An experiment is outlined with sample calculations to determine the actual screening ability in a superconductor. It is recognized that a superconducting medium for fusion energy extraction is not practical now, because transition temperatures are still too low. A specific analysis will address energy extraction abilities in a superconductor. To begin, the background of fusion cross sections will be discussed.

1.1 Fusion Cross Section

When combining lower binding energy nuclei, the excess binding energy of the combined nuclei is released as energy. This released energy far exceeds chemical energy release by about six orders of magnitude. However, the difficulty in releasing the energy from fusion events is that fusion requires that two positive charge nuclei combine against strong electrostatic repulsion. The repulsive barrier to fusion is known as the Coulomb barrier.

Coulomb repulsion can be characterized by a the potential energy [1]

$$U(r) = \frac{Z_1 \cdot Z_2 \cdot e^2}{4\pi\epsilon_o r} \tag{1}$$

where Z_n is the positive charge of particle n, e is the unit of charge (1.602×10^{-19} C), $\epsilon_o = 8.85 \cdot 10^{-12} \frac{\mathrm{F}}{\mathrm{m}}$ (or $1.417\,8 \times 10^{-30} \frac{\mathrm{C}^2}{\mathrm{m\,eV}}$) being the permittivity of free space, and r is the distance from the source charge.

Before the nuclei can overcome the Coulomb barrier, the nuclei (radii on the order of femtometers [$10^{-15}\,\mathrm{m}$]) must have a effective geometric probability of contacting each other (geometric cross section). If one nucleus tunnels through the barrier then the attractive nuclear forces help bring the nuclei together (Coulomb barrier transparency). Once the nuclei are inside the barrier, the probability of fusion is determined by experiment (astrophysical factor). The following equation summarizes the relevant physics.[2]

$$\sigma_f \approx \frac{S}{E} \cdot T \tag{2}$$

where σ_f is the fusion cross section (~probability of fusion), $\frac{1}{E}$ is the equivalent geometric cross section and E is center-of-mass energy, T is the Coulomb barrier transparency, and S is the astrophysical factor determined by experiment. It represents the likelihood of fusion given penetration of the coulomb barrier (S is dependent on energy).[2]

$$T = \exp\left(-\sqrt{\frac{\epsilon_G}{E}}\right) \tag{3}$$

where ϵ_G is the Gammow energy equal to $986.1 \cdot (Z_1 Z_2)^2 \, m_r/m_p$, where $m_r = (m_1 m_2) \,/\, (m_1 + m_2)$, and m_p is the mass of the projectile. The fusion reactions that will be discussed are deuterium-deuterium (D-D) and proton-boron (p-B) fusion. D-D fusion has two fusion product groups with near equal probability of occurring. Table 1 summarizes these reactions.[3]

Table 1. D-D and p-B Fusion Reaction Summary

Fusion Reaction	Reactants	Products (Energy [MeV])
$D-D$	${}_1^2H + {}_1^2H$	${}_1^1H[3.02] + {}_1^3H[1.01]$
		${}_2^3He[0.82] + {}_0^1n[2.45]$
$p-B$	${}_1^1H + {}_5^{11}B$	$3\left({}_2^4He\right)\,[8.68]$

1.2 Screening of Ions in Plasmas

Stars are able to utilize a plasma confinement mechanism that is not practical on Earth, namely gravity. Human life would not exist without fusion energy. With solar radiation, plants are able to synthesize food and generating oxygen, allowing life to flourish.

Astrophysicists study the stellar systems and the intricacies of formations and fusion reactions. An area of astrophysics that is not fully understood is how to explain why the neutrino flux from solar bodies is greater than the analytical predictions.[4] [5] These references offer an explanation that the enhancement in the fusion reaction rates is due to electron screening, which lowers the Coulomb barrier.

This screening effect is characterized by the Debye length (λ_D). Screening is only present when the Fermi electron velocity is greater than the fusion reactant velocity.[6] λ_D (now referred to λ for ease) is the distance between two charged particles before they can sense each other. For a Maxwell-Boltzman (MB) electron distribution in a plasma [7]

$$\lambda = \sqrt{\frac{\epsilon_o k_B T}{e^2 n_e}} \tag{4}$$

where e is the electron elementary charge, k_b is the Boltzmann constant, ϵ_o is the dielectric constant, n_e is the number density of the electrons, and T is the temperature. λ directly affects the transparency, T, in Eq. 3. When the screening effect is considered, T (transparency) becomes [2]

$$T \approx \exp\left(-\sqrt{\frac{\epsilon_G}{E + \epsilon_s}}\right) \tag{5}$$

where ϵ_s is the screening energy defined as [2]

$$\epsilon_s = \frac{Z_1 \cdot Z_2 \cdot e^2}{4\pi \cdot \epsilon_o} \cdot \frac{1}{\lambda} \tag{6}$$

If this screening effect is incorporated into Eq. 2 then [8]

$$\sigma_f = \frac{S\left(E+\epsilon_s\right)}{E+\epsilon_s} \exp\left(-\sqrt{\frac{\epsilon_G}{E+\epsilon_s}}\right) \tag{7}$$

Astrophysicists have been able to simulate electron screening in plasmas by utilizing metallic environments. In fact, metals have been referred to as the poor man's plasma.[8] [9]

1.3 Screening of Ions in Metals

Metals are more capable at electron screening than a substance with a M-B distribution of electrons in a substance. Metals contain conduction electrons that are able to relocate to regions with higher relative positive charge in order to effectively cancel out the higher relative charge. In doing so, the relative change in the charge distribution creates an enhanced Coulomb screening effect. Derivations [10] [11] of the screening ability start with Poisson's equation

$$\nabla^2 \Phi_{ind}(r) = 4\pi e[N(r) - N_0] \tag{8}$$

where Φ_{ind} is the induced potential, $N(r)$ is the induced electron density, and N_0 is the charge density prior to the addition of a conduction electron.

The electron energy changes according to the potential and the Fermi energy (ϵ_f).

$$\varepsilon(r) = \epsilon_f - e\Phi_{ind}(r) \tag{9}$$

This equation is set equal to the Fermi energy in the following equation [12]

$$N = \int_0^\infty \rho(E) f(E) dE \tag{10}$$

where $\rho(E)$ is the electron density of states

$$\rho(E) = \frac{8\sqrt{2}\pi m^{3/2}}{h^3} \tag{11}$$

and $f(E)$is the distribution function of the electron type, which is Fermi-Dirac for a conduction electrons in a metal.

$$f(E) = \frac{1}{e^{(E-\epsilon_f)/k_B T} - 1} \tag{12}$$

Solving Eq. 10 for ϵ_f and inputting the solution into Eq. 9. Then the combined equation is inserted into Eq.8 and the terms are rearranged to isolate Φ_{ind}

$$\nabla^2 \Phi_{ind}(r) = -\frac{1}{\lambda^2} \Phi_{ind}(r) \tag{13}$$

The coefficient to $\Phi_{ind}(r)$ becomes the negative inverse square of the screening length.

Putting the derivation in an easily applicable form [7]

$$\lambda_e = \sqrt{\frac{2}{3}\frac{\epsilon_o k_B T_F}{e^2 n_e}} \tag{14}$$

where n_e, or conduction electron density, can be calculated by [12]

$$n_e = \frac{8 \cdot \sqrt{2}\pi \left(m_e \cdot c^2\right)^{3/2}}{h_c^3} \left(\frac{2}{3}\epsilon_f^{3/2}\right) \tag{15}$$

and h_c is $\hbar \cdot c$, where c is the speed of light, which results in $h_c = 1240\,\mathrm{eV\,nm}$. The notable parameters are Fermi temperature (T_F) and electron density. The potential energy changes from Eq. 1 as follows [7]

$$U\left(r\right) = \frac{Z_1 \cdot Z_2 \cdot e^2 \exp\left(\frac{-r}{\lambda}\right)}{4\pi\epsilon_o r} \tag{16}$$

So one can infer that the $U \propto \exp\left(-1/\lambda\right)$ and $\lambda \propto T^{\frac{1}{2}}$. As $T_F \uparrow$ then $U \downarrow$ which is logical. The electrons will be traveling further away at any given time from the nucleus causing the screening to be spread out over a larger distance, rather than close to the nucleus where screening is more effective.

1.4 Screening of Ions in Superconductors

In metals the electrons flow with resistance due to scattering by other electrons and nuclei. However in superconductors, some electrons are able to flow with less resistance, because the electrons move in pairs called Cooper pairs.[13] Conduction electrons are able to pair, moving from Fermi-Dirac statistics to Bose-Einstein statistics. This transition is enabled once the superconductor drops below the critical temperature for superconductivity (T_c). Cooper pairs are typically spaced out over 10's to 100's of lattice constants. This spacing is known as the coherence length (ξ_o). Superconductors exhibit electric field expulsion which depends on how well a superconductor cancels out external electric fields. This field expulsion is characterized by the London penetration depth (λ_L). These parameters are experimentally derived. They can be used in calculations for electron screening.

Compared to conduction electrons (degenerate Fermions) in metals, the Cooper pairs following Bose-Einstein statistics have higher electron densities at the same energy level.[12] Based on the ease of Cooper pair movement and their statistics, it is unclear how superconductor electron screening would behave. Electric field screening in superconductors is not fully understood or agreed upon.[14] There have been claims that superconductor screening will be much greater than in metals, while others disagree.[15] [16] Stoppini and Shibata independently established theories for Cooper pair screening, where the pair can widen the Fermi energy band by two electron charges instead of one electron charge, as in ordinary metals.[7] [10] [17] This would result in more screening than seen in metals according to their theories. The Stoppini (PdD) and Shibata (metallic Hydrogen) derivation of λ_{sc} (superconductor Debye length) use similar techniques as shown for the λ_e derivation above. This increased screening has not been fully verified by experiment yet.[16] There has been an experiment performed to

measure the decay constants of O-19 in superconducting niobium.[18] The preliminary test results indicate weak superconducting screening, but the results have not been fully analyzed.

There is a clear and understood method of determining the number density of Cooper pairs (n_c), which may be useful in determining the contribution of Cooper Pair screening.[10]

$$n_c = \frac{\varepsilon_o m_e c^2}{\lambda_L^2 e^2} \tag{17}$$

1.5 Screened Cross Sections

Typical λ and ϵ_s values are outlined in Table 2. The range of λ and ϵ_s for superconductors are derived from Stoppini's and Shibata's work with the consideration that screening values may in fact be no greater than ordinary metals. The screening in an insulator is comparable to the radius of an atom.[19] The superconductor screening values are inferred from pessimistic and optimistic predictions.[7] [15] [16] [17] [18]

Table 2. Screening Energies

	Insulator	Metal	Superconductor
$\lambda\,(m)$	$10^{-10} - 10^{-9}$	$10^{-11} - 10^{-10}$	$10^{-13} - 10^{-10}$
$\epsilon_s(eV)$	$10s$	$100s$	$100s - 1,000s$

With screening energies defined, it is possible to show the effects of screening on fusion cross sections. D-D fusion will be used as an example ($\epsilon_G = 986 \times 10^3\,\mathrm{eV}$ and $S \approx 2 \cdot 5 \times 10^4\,\mathrm{eV\,b}$ to account for the two main branches of D-D fusion).[2] [20] Given that the enhancement levels are less than 1 keV, the S-factor would vary minimally for D-D fusion at that low energy level.[20]

Using Eq. 6 and 7, where $\epsilon_o = 1.417\,8 \times 10^{-30}\,\frac{\mathrm{C^2}}{\mathrm{m\,eV}}$, Z_1 and $Z_2 = 1$, the fusion cross section (σ_f) is plotted in Fig. 1 with varying screening values (λ). Fig. 1 agrees with the understanding that σ_f will only go as low as the σ_f for ϵ_s. $\epsilon_s \approx 0.1keV$ for $\lambda = 10^{-11}\,\mathrm{m}$ and $\epsilon_s \approx 1keV$ for $\lambda = 10^{-12}\,\mathrm{m}$.

Another useful comparison is to see how the ratio of σ_f to (σ_c (Coulomb scattering) + σ_f) changes with screening. σ_c is defined for large angle Coulomb scattering as [21]

$$\sigma_{DD} = \frac{6.4 \times 10^{-2}}{E_D^2}\,[barns] \tag{18}$$

where E_D is the center of mass kinetic energy of the deuterons in eV. The ratio $\sigma_f/\left(\sigma_c + \sigma_f\right)$ represents the likelihood of a fusion given a collision with the simplifying assumption that $(\sigma_c + \sigma_f)$ represents the total D-D cross section. $\sigma_f/\left(\sigma_c + \sigma_f\right)$ is shown in Fig. 2. Note that small angle Coulomb scattering is not covered in this graph or equation. Above ~2 keV $\sigma_f/\left(\sigma_c + \sigma_f\right) = 1$.

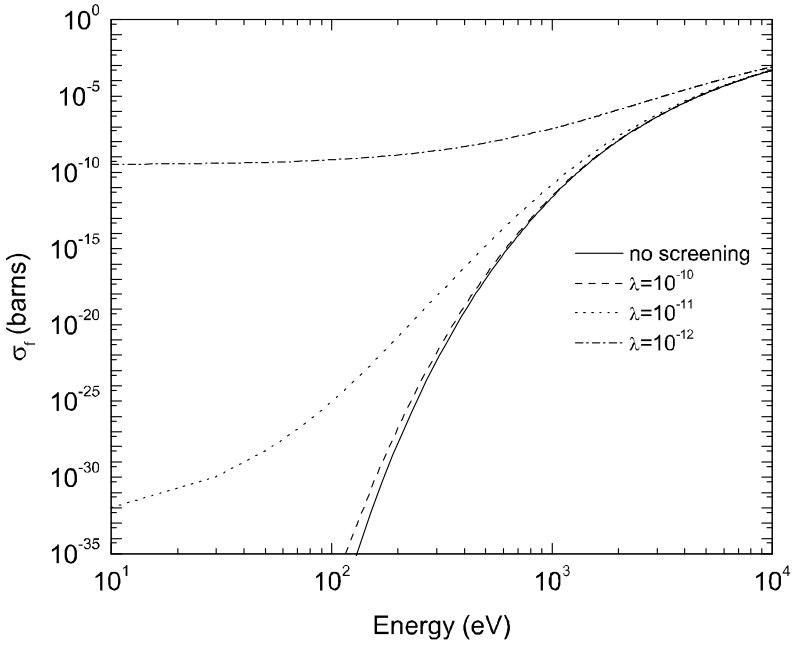

Figure 1. Screening Effect on D-D Fusion Cross Section

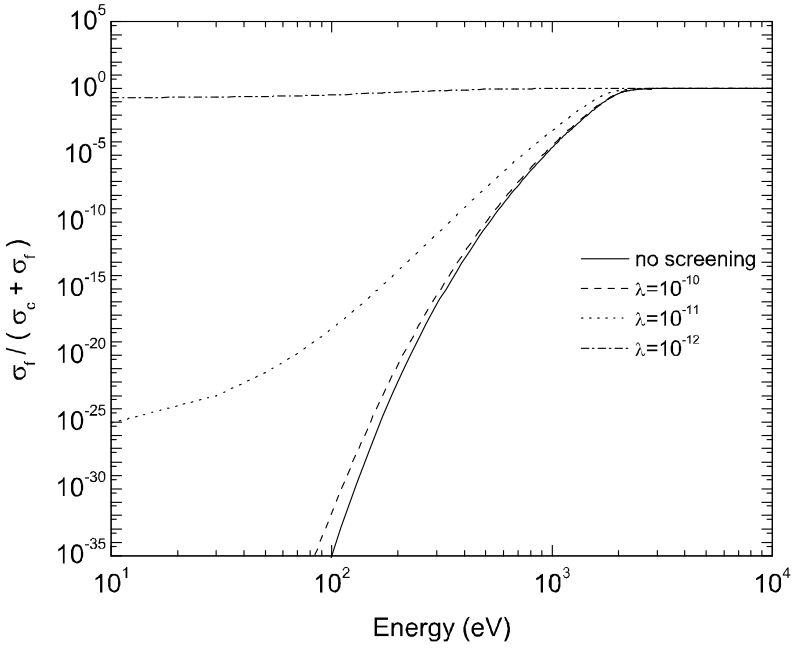

Figure 2. Screening Effect on D-D Cross Section Ratios

Chapter 2
Superconducting Materials

This chapter considers superconducting materials that could potentially be used to better understand screening of fusion reactions. The two materials considered are Palladium Deuteride (PdD) and Magnesium Diboride (MgB_2).

2.1 Palladium Deuteride

2.1.1 Background

Palladium has the ability to take hydrogen isotopes into solid solution very easily. Hydrogen then is able to diffuse easily within the lattice.[22] As palladium takes up more hydrogen the properties of the resulting PdH_x takes on interesting properties. The relative resistance of the PdH_x increases up to x=0.78 and then decreases rapidly to x=1 (Fig. 3).

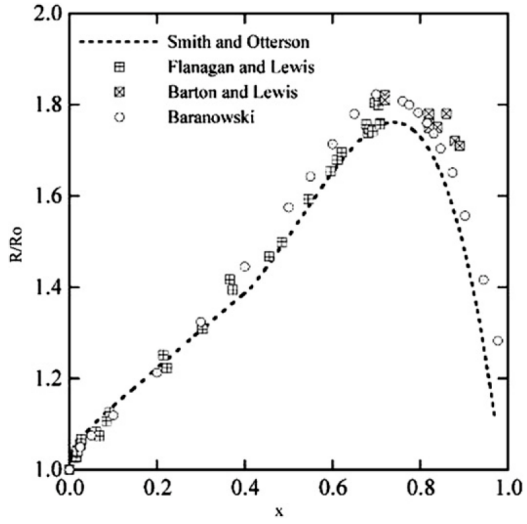

Figure 3. Relative Resistance of PdH Loading. Source: (Tripodi, P. et al. The effect of hydrogen stoichiometry on palladium strain and resistivity. Physics Letters A 373, 4301–4306(2009).)

PdH_x becomes a superconductor with a 1-2 K transition temperature once the loading of hydrogen is greater than ~0.75. As the loading increases above ~0.75 the transition temperature to superconductivity increases as shown in Fig. 4. When hydrogen is replaced with deuterium, T_c increases for a given hydrogen loading. This is an atypical relationship for superconductors.

As shown in Fig. 5, when the PdH_x is exposed to a dose of hydrogen T_c increases as the

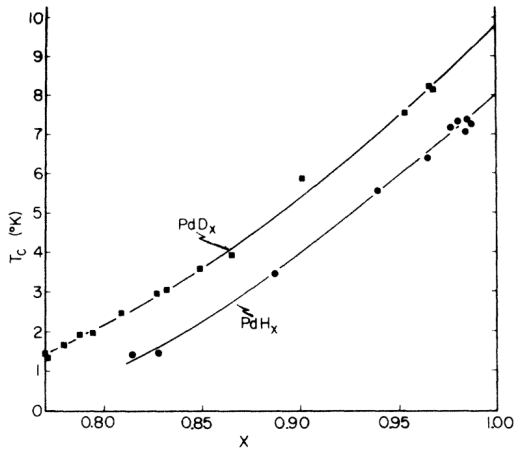

Figure 4. T_c as a Function of Loading. Source: (Schirber, J. & Northrup, C. Concentration dependence of the superconducting transition temperature in PdHx and PdDx. Phys. Rev. B 10, 3818–3820(1974).)

loading increases until the dose begins to degrade the superconductivity of the material.

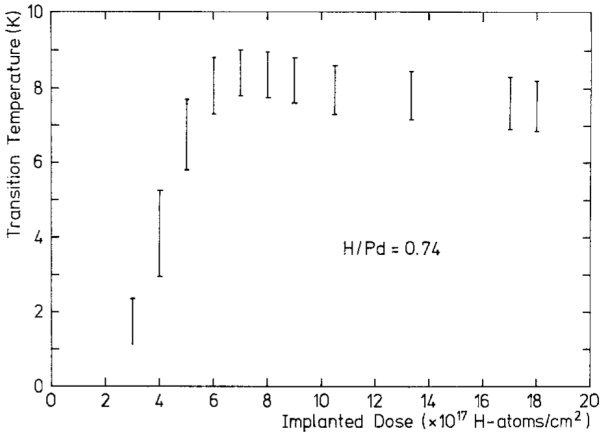

Figure 5. T_c as a Function of Dose. Source: (Heim, G. & Stritzker, B. Ion Implantation A Powerful Technique for the Production of Metastable Superconducting Alloys. Appl. Phys.7, 239 248(1975).)

Stoppini theorized that there would be a "superscreening" effect that PdD Cooper pairs would exhibit, which would enhance σ_f.[17] Stoppini's derivation seeks to explain the screening effect of Cooper pairs. Stoppini claims that both electrons participate in screening. This will require that Cooper Pairs (separated by ~100 Å) would exist long enough in close proximity to the nuclei to screen incoming ion repulsion. Stoppini calculates the formation of Cooper pairs by using boson condensation.

Using Eq. 15, the conduction electron density is $n_e = \frac{1.047\times10^{29}}{\mathrm{m}^3}$. Stoppini derived the

relationship between temperature and Cooper pairs.[17]

$$n_c(T) = \frac{n_e}{2}\left(1 - \left(\frac{T}{T_c}\right)^4\right) \tag{19}$$

Then the Debye wavelength for the Cooper pairs was derived.

$$\lambda_c(T) = 5.8 \times 10^{-11}\sqrt{\frac{T/T_c}{1-(T/T_c)^4}}\,\mathrm{cm} \tag{20}$$

Combining the Debye wavelength for the Cooper pairs and conduction electrons, the effective λ is

$$\lambda(T) = \left(\frac{g(T)}{\lambda_c(T)} + \frac{1-g(T)}{\lambda_e}\right)^{-1} \tag{21}$$

where $g(T) = \frac{n_c(T)}{n_e}$. In Table 3, sample calculated values of n_c, g, and λ are presented.

Table 3. PdD Superconducting Characteristics based on Stoppini's Derivation

	$n_c\left(\mathrm{m}^{-3}\right)$	g	$\lambda(m)$
3K	5.2×10^{28}	0.50	6.1×10^{-13}
5K	5.0×10^{28}	0.48	8.3×10^{-13}
10K	1.7×10^{28}	0.15	5.6×10^{-12}
$>\mathrm{T}_c$	0	0	5.3×10^{-11}

These proposed values of λ would have a large effect on σ_f as shown in Fig. 1.

2.1.2 PdH: A High Temperature Superconductor?

Electrolytic loading of deuterium in palladium has shown signs of high temperature (near room temperature) superconductivity when loading was greater than unity.[23] [24] While there is evidence of superconducting signatures (e.g., magnetic susceptibility, critical currents, and resistance drops when T goes below T_c), criticisms have been made and rebutted.[25] [26] For example, the relative resistance drops when $T < T_c$ shown in these highly loaded PdH experiments is not as large as other superconductors (i.e., MgB_2). An Additional PdH theory has been published on the existence of heavy bosons (deuterium) contributing to superconductivity or non-equilibrium existence of superconducting states at high temperatures (from high acoustic plasmon frequencies).[27]

However, according to Stritzker in 1975, with a maximum loading of x=1.3 the maximum T_c for PdD only reached 10.7K leading one to question Tripodi's studies. However, as the dose/loading increases, the T_c dropped as shown by Heim and Stritzker.[28] Additionally, the estimations of hydrogen loading do not appear to be rigorous across all experiments in the field. The interpretation of how many deuterons are taken up by the material is difficult with ion implantation and deuteron diffusion. It is possible, as Tripodi proposes, that there are regions of superconductivity that are masked by non-superconducting regions.[23] Despite several studies over many years, the superconductivity within PdD is still contentious.

Nonetheless, it is a good candidate for experiments to study the effects of D-D fusion rates especially with the prospect of increased screening and T_c. An additional superconductor that may be considered for Cooper pair screening for fusion reactions is magnesium diboride.

2.2 Magnesium Diboride

In 2001, magnesium diboride (MgB_2) was discovered to have superconducting properties.[30] MgB_2 is especially appealing for current carrying applications, since it is the highest known metallic superconductor. The T_c for MgB_2 is $39\,\mathrm{K}$.[30] MgB_2 is the highest T_c superconductor identified that contains the fusion reactant of boron. Boron-11 would be the isotope required in MgB_2 in order to enable fusion reactions with hydrogen. There has yet to be a derivation or explanation of the screening of the Coulomb barrier for MgB_2. This may offer another material to test to determine the effects of superconductivity on fusion reaction rates, like p-B fusion. Now consider what the effects of screening could have on fusion reaction rates.

Chapter 3
Reaction Rates

3.1 General Framework

There are two possible ways to consider reaction rates in a superconductor. Reaction rates can be calculated either by the lattice vibration of nuclei or by external ions impinging the superconductor. Where the reaction rate is well known for external ion induced fusion, lattice vibration induced fusion reaction rates have been debated.

First, the reaction rate formulation for vibration induced fusion will be discussed. The formula will need to include σ_f from Eq. 7 reduced by the possible vibration directions. Additionally, the number of available reactants and the frequency of collisions must be included. The result is

$$R_0 = \frac{\omega_D}{2\pi} \cdot N \cdot N_n \cdot \frac{\sigma_f}{4\pi a^2} \tag{22}$$

where ω_D is the Debye frequency (lattice vibration frequency). Then $\frac{\omega_D}{2\pi}$ is the inverse of the oscillation period. N is the number density of reactants (e.g., deuterons), N_n is the number of nearest neighbors, and a is the lattice constant. $4\pi a^2$ is the spherical area of possible vibration directions. Expanding this equation,

$$R_1 = \frac{\omega_D}{2\pi} \cdot \frac{N \cdot N_n \cdot S}{k_B T + \epsilon_s(T)} \cdot \frac{1}{4\pi a^2} \exp\left(-\sqrt{\frac{\epsilon_G}{k_B T + \epsilon_s(T)}}\right) \tag{23}$$

Second, the reaction rate formulation for external ion inducing fusion will be discussed. As an ion enters the superconductor it slows down, which changes σ_f. The energy (and later calculated σ_f) decrease as a function of penetration depth, which can be inferred from the code SRIM.[29] By using Eq. 7 (σ_f) and the energy as a function of depth, $\sigma_f(x)$ can be integrated to obtain σ_i (units of distance cubed).[31] Therefore, the reaction rate is defined as

$$RR = N \cdot \sigma_i \cdot I \tag{24}$$

where I is the number of ions per second striking the target at the energy that σ_i is based upon. An alternate means of calculating reaction rates are provided in the following reference.[32]

These two methods of inducing fusion are different, because external ions in Eq. 24 are only considered able to fuse while their energy remains above the vibration energy of the material. With vibration induced fusion, the nuclei in the lattice will continue to attempt to fuse at vibration energies.

3.2 Parametric Study of PdD

This section considers what the expected PdD vibration induced fusion rates would be with different screening lengths. The density of PdD is determined by the lattice spacing of the

Pd in the Face-Centered Cubic (FCC) structure, $a = 4.0\,\text{Å}$.[34] Because there are four D atoms and four Pd atoms per site the number density D and Pd are $n_{Pd} = n_D = \frac{4}{(4.0\,\text{Å})^3} = 6.25 \times 10^{28}\,\text{m}^{-3}$

$\omega_D = 6 \times 10^{12}\,\text{Hz}$,[22] which can alternately be defined by [13]

$$\omega_D = \frac{\Theta_D k_b}{h_b} \tag{25}$$

where $\Theta_D = 285\,\text{K}$ for PdD [33]

For the specific case of PdD, reductions in the reaction rate must be accounted for due to theoretical deuteron mobility and boson formation.[17] [34] Only the excited fraction in a boson fluid can participate in a fusion process. The excited fraction reduces as temperature drops below the boson condensation temperature of deuterons. This fraction of excited deuterons is defined as[17]

$$f_1 = 2\,(T/T_\lambda)^{5.6} \tag{26}$$

where $T_\lambda = 13.4\,\text{K}$, which is the condensation temperature of deuterons. If $T > T_\lambda$ then f_1 is neglected, because no formation of deuteron bosons is possible.

For PdD in a non-superconducting state, only the fraction of the deuterons that diffuse are able to interact with other deuterons.[34]

$$f_2 = \exp\left(-\left[\Delta\Phi - 3/2 h_b\sqrt{\Phi''/m_D}\right]/\,(k_b T)\right) \tag{27}$$

where $m_D = 1875.6\,\text{MeV}/c^2$, and $c \approx 3 \times 10^8\,\text{m/s}$. $\Delta\Phi = 0.23\,\text{eV}$ is the barrier height between minima, and $\Phi'' = 1.1\,\text{eV}\,\text{Å}^{-2}$ is the curvature of the local minima of the lattice (both for PdD).[34] While Ichimaru's [34] reaction rate formulation includes this reduction factor, Stoppini does not. This factor accounts only for the non-superconducting state's ability of deuterium to tunnel to another occupied deuterium site in the lattice thus enabling attempted fusion. This does not account for the ability of conduction electrons or Copper pairs to screen the barrier height. The incompleteness of this equation must be considered when evaluating the reaction rate results. Combining the factors for PdD, the reaction rate becomes

$$R_2 = R_1 f_1 f_2 \tag{28}$$

Table 4 is obtained by using Stoppini's derivation of λ and the Section 1.5 D-D parameters. The last column includes a reaction rate (R_s) calculated in Stoppini's article. Stoppini's calculation provides another means of finding the transparency (T), which are not in agreement with alternate references.[2] [20] If Tripodi's experiments are fully validated, then the third row (266 K) in Table 4 is obtained by taking the critical temperature of PdD (x$\gg$1) to be room temperature. For simplicity, the calculation for x$\gg$1 in the third row uses the same lattice spacing and density as the x=1 calculations. The fourth row shows the D-D reaction rate at room temperature in non-superconductor PdD. While there appear to be experiments that could have provided validation for superconductor reaction rates, the specific parameters and results do not validate or invalidate the theorized superconductor screening ability discussed. Tests were performed to observe the reaction rates from ion loading of Pd with D at low temperatures (1.5 keV D^+ from 40-330K). No charged particles were detected with loading ratios that were no lower than x=0.56.[35] Therefore, it is possible that the material never

Table 4. PdD Reaction Parameters

T	T/T_c	$\epsilon_s(\mathrm{eV})$	f_1	f_2	$R_2(\mathrm{m}^{-3}\cdot s^{-1})$	$R_s(\mathrm{m}^{-3}\cdot s^{-1})$
5 K	$5/11$	8655	0.0080	$3.0\cdot 10^{-160}$	$\tilde{}10^{-133}$	$3\cdot 10^{8}$
10 K	$10/11$	1272	0.39	$1.7\cdot 10^{-80}$	$\tilde{}10^{-53}$	$--$
266 K	$266/293$	1272	$--$	$1.0\cdot 10^{-3}$	$2.3\cdot 10^{18}$	$--$
293 K	>1	144	$--$	$1.9\cdot 10^{-3}$	$5.3\cdot 10^{-5}$	$--$

was able to become a superconductor. This would prevent a valid comparison between experimental data and the R_2 and R_s reaction rates. In superconductivity tests below T_c no known attempts were made to observe reactions from fusion. For experiments with fusion product detectors, temperatures were above T_c in reported cases. This leaves a gap in verifying fusion reaction rates in superconductors.

Chapter 4
Scientific Experiment Concept

Given the uncertainty of the screening length in superconductors, an experiment is warranted to compare the theory of Stoppini and Shibata. Chapter 3 showed considerable vibration induced reaction rate density using the predictions of Stoppini and Tripodi. This chapter advances the concept of an experiment to determine screening lengths. It provides detailed numerical estimates of possible experimental parameters.

4.1 Determining the Screening Energy in PdD and MgB_2

To begin, the general experimental guidelines for determining ϵ_s are discussed followed by quantitative details. For PdD, a thin Pd sample should be prepared for exposure to low energy deuterons. Upon loading high enough to reach superconductivity, the reaction rate from Eq. 24 should be calculated to predict reaction rates for given ϵ_s's. The experiment should also be performed with a small enough sample such that the vibration induced reaction rate would be negligible. The experiment must have enough ion induced fusion products detected above the background to enable enough resolution to determine ϵ_s. To determine if actual fusion reactions are taking place with 95% confidence, the detected counts have to be greater than the error in background and detected counts [36]

$$cts - B = 4.653\sigma_B + 2.706 \tag{29}$$

where cts are the total number of counts, B is the number of background counts, σ_B is the standard deviation of the background counts ($\sigma_B = \sqrt{B}$). The standard deviation of values can be reduced by performing multiple experiments, which lowers counting σ's by square root of the average counts over the number of independent counts $\sqrt{\frac{\overline{cts}}{N}}$.[36] N is the number of experiments performed with the same experimental parameters.

Once the counts of fusion products are declared above background, the resolution of the desired ϵ_s depends on the uncertainty of the number of counts obtained. The 95% confidence interval ($x \pm 1.96\sigma$ or $cts \pm 1.96\sqrt{cts}$)[36] of the detected counts will determine the uncertainty of the screening energy (ϵ_s). The screening energy is determined by comparing the observed fusion product counts at the detector to the precalculated reaction rates calculated by Eq. 24.

Using the formulation which demonstrates combinations of screening energies, the Cooper pair contribution to ϵ_s can be determined based on the total screening energy (equation modified for this application) [37]

$$\epsilon_{s\_sc} = \left(\epsilon_s^2 - \epsilon_{s\_metal}^2\right)^{1/2} \tag{30}$$

where ϵ_{s_sc} is the screening energy of Cooper pairs in the superconductor, ϵ_{s_metal} is the contribution from λ_e from Eq. 14, and ϵ_s is the total screening energy. A sample sequence of testing is outlined in Table 5. For a more accurate method of determining ϵ_{s_metal} than

Eq. 14, the test sequence includes testing above the critical temperature. This is important, because testing two out of the three terms in Eq. 30 will establish an accurate means of finding the superconducting contribution to the screening energy, ϵ_{s_sc}.

Table 5. Test Sequence

Temperature	T_1	T_2	T_3
Temperature range	$> T_c$	$< T_c$	$<< T_c$
Fusion product counts	cts_1	cts_2	cts_3
Calculate reaction rate	RR_1	RR_2	RR_3
Calculate ϵ_{s_sc}	ϵ_{s_sc1}	ϵ_{s_sc2}	ϵ_{s_sc3}

With MgB_2, a similar process should be used with the P-B fusion reaction shown in Table 1. Where implantation of deuterium with PdD increases the critical temperature of the superconductor, the effects of hydrogen on MgB_2 will have to be investigated prior to an experiment. An MgB_2 experiment would offer a unique perspective on Cooper pair screening given the presence of inner orbital electrons, in contrast with deuterons in PdD.

4.1.1 Sample PdD Calculation

This section quantitatively outlines how the screening energy can be deduced from the detection of fusion products.

An assumption in this calculation is that the number of implanted deuterons are negligible compared to the starting number of deuterium in the PdD lattice. Reaction rates for two different incoming D^+ ions (20 keV and 150 keV) will be considered with varying degrees of screening. The reaction rate for externally accelerated ions, as discussed in Chapter 3, requires that σ_i be calculated. When accounting for the additional screening energy, σ_i becomes

$$\sigma_i = \int_{d_i}^{d_m} \sigma_f\left(\epsilon_s, x\right) dx \tag{31}$$

where d_m is the maximum depth of deuteron ions and d_i is the initial depth at which the ions start. For 20 keV deuterons in this example, σ_i represents the integrated cross section of the fusion reaction that results in 3.02 MeV protons (i.e., S-factor at average energy of ~10 keV in PdD is 58.6 ± 0.6 keV-barns)[38] . The fusion protons will be the subject of detection in this sample calculation. The numerical form of this equation is

$$\sigma_i = \left(5.89 \times 10^4 \pm 600\right) \cdot 10^{-38}\,\mathrm{m}^3 \int_0^{1060} \frac{\exp\left(-20\sqrt{2465}\sqrt{\frac{1}{\epsilon_s - 1000(0.018\,5x - 19.\,66)}}\right)}{\epsilon_s - 1000\left(0.018\,5x - 19.\,66\right)} dx \tag{32}$$

where ϵ_s is in eV and σ_i is in m^3. Sample values of ϵ_s and λ with their subsequent σ_i and $\sigma_i N_D$ values are shown in Table 6 (20 keV deuterons), where $N_D = 6.25 \times 10^{28}/\,\mathrm{m}^3$. $\sigma_i N_D$ represents the probability of fusion with proton emission given the bombardment of one deuteron at the prescribed energy.

For the sample calculation, an imposed limit on deuteron implantations is set to a 1% change

Table 6. Precalculated Integrated Fusion Cross Section at 20 keV

$\epsilon_s(\mathrm{eV})$	$\lambda(\mathrm{m})$	$\sigma_i\left(\mathrm{m}^3\right)$	$\sigma_i N_D$ (unitless)
0	–	$6.71 \times 10^{-39} \pm 7 \times 10^{-41}$	$4.19 \times 10^{-10} \pm 4 \times 10^{-12}$
200	3.6×10^{-11}	$6.98 \times 10^{-39} \pm 7 \times 10^{-41}$	$4.36 \times 10^{-10} \pm 4 \times 10^{-12}$
400	1.8×10^{-11}	$7.26 \times 10^{-39} \pm 7 \times 10^{-41}$	$4.54 \times 10^{-10} \pm 5 \times 10^{-12}$
600	1.2×10^{-11}	$7.55 \times 10^{-39} \pm 8 \times 10^{-41}$	$4.72 \times 10^{-10} \pm 5 \times 10^{-12}$
800	9.0×10^{-12}	$7.85 \times 10^{-39} \pm 8 \times 10^{-41}$	$4.91 \times 10^{-10} \pm 5 \times 10^{-12}$
1000	7.2×10^{-12}	$8.16 \times 10^{-39} \pm 8 \times 10^{-41}$	$5.10 \times 10^{-10} \pm 5 \times 10^{-12}$
1250	5.7×10^{-12}	$8.55 \times 10^{-39} \pm 9 \times 10^{-41}$	$5.34 \times 10^{-10} \pm 5 \times 10^{-12}$
1500	4.8×10^{-12}	$8.95 \times 10^{-39} \pm 9 \times 10^{-41}$	$5.59 \times 10^{-10} \pm 6 \times 10^{-12}$
1750	4.1×10^{-12}	$9.36 \times 10^{-39} \pm 1 \times 10^{-40}$	$5.85 \times 10^{-10} \pm 6 \times 10^{-12}$
2000	3.6×10^{-12}	$9.79 \times 10^{-39} \pm 1 \times 10^{-40}$	$6.12 \times 10^{-10} \pm 6 \times 10^{-12}$
3000	2.4×10^{-12}	$1.16 \times 10^{-38} \pm 1 \times 10^{-40}$	$7.26 \times 10^{-10} \pm 7 \times 10^{-12}$
5000	1.4×10^{-12}	$1.58 \times 10^{-38} \pm 2 \times 10^{-40}$	$9.90 \times 10^{-10} \pm 1 \times 10^{-11}$

in the loading in order to prevent changes in critical temperature as discussed in Chapter 2. For 20 keV deuterons in PdD with x=1, SRIM shows deuterons would implant between the surface and ~1000 Å. Lateral straggling is neglected for simplicity. The initial number of deuterons in PdD with x=1 is

$$D_{initial} = N_D \cdot 1000\,\text{Å} \cdot A \tag{33}$$

where A is the chosen area of deposition. For this example an area of 10 mm^2 is chosen as the beam width, which results in $D_{initial} = 1000\,\text{Å} \cdot 6.25 \times 10^{28}/\,\mathrm{m}^3 \cdot 10\,\mathrm{mm}^2 = 6.25 \times 10^{16}$ deuterons. For the loading to not change more than 1%, the limit on implanted deuterons is 6.25×10^{14} (D_{limit}). This dose of deuterons is less than the dose in Fig. 5, which showed that superconductivity was not deteriorated by the dose.

Now consider what resolution of screening energy can be determined by the limit on the number of deuterons allowed to be projected at the surface. If the screening energy is assumed to be 400 eV, then the resolution of screening energy can be determined in the following way. This calculation assumes that the background counts in the time of the experiment are negligible. Out of the D_{limit} deuterons that enter PdD, the number of resulting fusion events with proton emission is $D_{\text{limit}} \cdot \sigma_i N_D = 6.25 \times 10^{14} \cdot \left(4.54 \times 10^{-10} \pm 5 \times 10^{-12}\right) = 2.84 \times 10^5 \pm 3000$. To determine how many protons can be detected, a sample detection system will be discussed. This sample detection system modeled is similar to a Passivated Implanted Planar Silicon (PIPS) with a near 100% detection efficiency of protons (H-1 at 3.02 MeV) that impinge the detector. The detector is assumed to be 3 cm^2 at a distance of 4 cm from the PdD fusion site. This results in a detection efficiency of protons emitted of [36]

$$\eta_{\text{det}} = \frac{\eta_{int}\Omega}{4\pi} \tag{34}$$

where η_{int} is the intrinsic detector efficiency given a proton striking the detector ($\eta_{int} = 1$ for this example) and Ω is the solid angle relating detector to source distances and sizes. For a circular detector (radius a) at a distance d from the source [36]

$$\Omega = 2\pi\left(1 - \frac{d}{\sqrt{d^2 + a^2}}\right) \tag{35}$$

where $a = \sqrt{3\,\mathrm{cm}^2/\pi} = 0.977\,\mathrm{cm}$, and this results in $\Omega = 0.18$.

Therefore, $\eta_{\mathrm{det}} = 0.014$. So η_{det} times the total proton emission events (2.84×10^5) is $0.014 \cdot 2.84 \times 10^5 = 3980$, which is the total protons that will be counted. Because these are physically counted events, the error is calculated separate from the theoretical error on proton emissions mentioned previously (i.e., 3000). The standard deviation is equal to $\sigma_{cts} = \sqrt{3980} = 63.1$. To determine what the error is associated with the actual 400 eV screening energy, the reverse process of this calculation must be performed for the upper and lower range of the possible counts. To determine the range of $\epsilon_s$the following steps are performed to find:

(1) Proton counts
(2) Protons emitted from PdD from fusion
(3) Fraction of ions resulting in fusion (i.e., $(\sigma_i N_D)_{\mathrm{exp}}$, which is the calculated value of $\sigma_i N_D$ based on the experiment)
(4) Screening energy

If there are errors in the experimental execution (e.g., total deuterons impinged on target), then the third step will have to include these additional uncertainties. Additionally, the error contribution of the background counts will have to be propagated through. Progressing the error from steps 1-3, the error on $(\sigma_i N_D)_{\mathrm{exp}}$ is written as

$$\sigma_{\_}(\sigma_i N_D)_{\mathrm{exp}} = \sigma_{cts} \cdot \frac{1}{\eta_{\mathrm{det}}} \cdot \frac{1}{D_{\mathrm{limit}}} \tag{36}$$

which results in $\sigma_{\_}(\sigma_i N_D)_{\mathrm{exp}} = 7.21 \times 10^{-12}$. So the experimental $(\sigma_i N_D)_{\mathrm{exp}} = 4.54 \times 10^{-10} \pm 7 \times 10^{-12}$. The 95% confidence $(\sigma_i N_D)_{\mathrm{exp}}$ lower bound is $4.54 \times 10^{-10} - 1.96 \cdot 7 \times 10^{-12} = 4.40 \times 10^{-10}$ and upper bound is $4.54 \times 10^{-10} + 1.96 \cdot 7 \times 10^{-12} = 4.68 \times 10^{-10}$. The 95% confidence interval on the actual screening energy of 400 eV is ~200 eV to ~600 eV judging from Table 6. This is a seemingly unacceptable error. If 150 keV deuterons were used with same D_{limit}, the range of ϵ_s would be even greater due to the closer proximity between $\sigma_i N_D$ values. However, with 150 keV deuterons the D_{limit} would be 2-3 times greater due to larger penetration depths. To decrease the size of the confidence interval of the 20 keV experiment, a larger detection area or a higher D_{limit} could be used. Expanding Eq. 36 below

$$\sigma_{\_}(\sigma_i N_D)_{\mathrm{exp}} = \sqrt{\eta_{\mathrm{det}} \cdot D_{\mathrm{limit}} \cdot \sigma_i N} \left(\frac{1}{\eta_{\mathrm{det}}} \cdot \frac{1}{D_{\mathrm{limit}}} \right) \tag{37}$$

The improvement on the $\sigma_{\_}(\sigma_i N_D)_{\mathrm{exp}}$ can be shown as

$$\sigma_{\_}(\sigma_i N_D)_{\mathrm{exp}} \propto \frac{\sqrt{\eta_{\mathrm{det}} D_{\mathrm{limit}}}}{\eta_{\mathrm{det}} D_{\mathrm{limit}}} \tag{38}$$

By increasing the loading limit from 1% to 5% and increasing the detection efficiency by 4 times (e.g., closer or more detectors) the $\sigma_{\_}(\sigma_i N_D)_{\mathrm{exp}}$ can be reduced by a factor of $\sqrt{20}/20$. An increase from 1% to 5% loading is reasonable, because a 5% loading change around x=1 would only change T_c by a couple degrees Kelvin (see Fig. 4). The resulting $\sigma_{\_}(\sigma_i N_D)_{\mathrm{exp}}$ becomes $\sqrt{20}/20 \cdot 7.21 \times 10^{-12} = 1.61 \times 10^{-12}$. Interpolation from Table 6 to find the

screening energy is determined with

$$\epsilon_{s\_int} = \epsilon_{s\_low} + \frac{\epsilon_{s\_high} - \epsilon_{s\_low}}{(\sigma_i N_D)_{high} - (\sigma_i N_D)_{low}} \left[(\sigma_i N_D)_{\exp} - (\sigma_i N_D)_{low} \right] \tag{39}$$

where ϵ_{s_int} is the interpolated value of ϵ_s, $x_{\_low}$ and $x_{\_high}$ represent the lower and upper values of $\sigma_i N_D$ and ϵ_s (corresponding to 200 eV and 400 eV or 400eV and 600 eV) in Table 6, and $(\sigma_i N_D)_{\exp} = 4.54 \times 10^{-10}$ for this example. ϵ_{s_int} is exactly 400 eV in this example. But the error that comes from the experiment will propagate through this formula, which decreases the accuracy of the calculated screening energy. The errors in Eq. 39 are contained in each $(\sigma_i N_D)_x$ value (*x* represents high, low, and exp). The quadrature addition method [36] can be used to find the error of $(\sigma_i N_D)_{high} - (\sigma_i N_D)_{low}$ and $(\sigma_i N_D)_{\exp} - (\sigma_i N_D)_{low}$. Then the error of those two items can be combined by using error propagation for division [36] and multiplication by a constant. Putting these errors together, the resulting error on ϵ_{s_int} is

$$\sigma\_\epsilon_{s\_int} = (\epsilon_{s\_high} - \epsilon_{s\_low}) \cdot \sqrt{\frac{\left[\sigma\_(\sigma_i N_D)_{\exp}\right]^2 + \left[\sigma\_(\sigma_i N_D)_{hl}\right]^2}{\left[(\sigma_i N_D)_{high} - (\sigma_i N_D)_{low}\right]^2} + \left(\frac{\left[(\sigma_i N_D)_{\exp} - (\sigma_i N_D)_{low}\right]^2 2\left(\sigma\_(\sigma_i N_D)_{hl}\right)^2}{\left[(\sigma_i N_D)_{high} - (\sigma_i N_D)_{low}\right]^4} \right)} \tag{40}$$

This formulation assumes that the errors of $(\sigma_i N_D)_{high}$ and $(\sigma_i N_D)_{high}$ take on the highest value of the range of interpolation (represented by $\sigma\_(\sigma_i N_D)_{hl}$ in the equation). So between 200 eV and 400 eV or 400 eV and 600 eV the standard deviation on $(\sigma_i N_D)_{high}$ and $(\sigma_i N_D)_{low}$ is taken to be $\sigma\_(\sigma_i N_D)_{hl} = 5 \times 10^{-12}$. Between 200 eV and 400 eV the 95% confidence band is $\sigma\_\epsilon_{s\_int} \cdot 1.96 = 192$ eV. Between 400 eV and 600 eV the 95% confidence band is $\sigma\_\epsilon_{s\_int} \cdot 1.96 = 114$ eV. The resulting 95% confidence interval for ϵ_{s_int} is 400^{+114}_{-192} or 209 eV to 514 eV (average $\pm 95\%$ error is 152 eV or 38% of 400 eV). If there were no error on the unscreened experimental S-factor (i.e., 58.6 ± 0.6 keV-barns)[38] , then the 95% confidence interval would be about 360 eV to 440 eV.

Once the screening energy from the experiment is determined, then the superconducting contribution to the screening energy can be extracted by using the metallic screening energy from the proposed experiment above T_c and Eq. 30. To determine the error of ϵ_{s_sc} based on the general form of error propagation [36]

$$\sigma^2_{\epsilon_{s\_sc}} = \left(\frac{\delta\epsilon_{s\_sc}}{\delta\epsilon_s} \right)^2 \sigma^2_{\epsilon_s} + \left(\frac{\delta\epsilon_{s\_sc}}{\delta\epsilon_{s\_metal}} \right)^2 \sigma^2_{\epsilon_{s\_metal}} \tag{41}$$

where $\epsilon_{s\_sc} = \left(\epsilon_s^2 - \epsilon^2_{s\_metal}\right)^{1/2}$ from Eq. 30, $\frac{\delta\epsilon_{s\_sc}}{\delta\epsilon_s} = \epsilon_s \left(\epsilon_s^2 - \epsilon^2_{s\_metal}\right)^{-1/2}$, and $\frac{\delta\epsilon_{s\_sc}}{\delta\epsilon_{s\_metal}} = -\epsilon_{s\_metal} \left(\epsilon_s^2 - \epsilon^2_{s\_metal}\right)^{-1/2}$. So the final $\sigma_{\epsilon_{s\_sc}}$ for ϵ_{s_sc} becomes

$$\sigma_{\epsilon_{s\_sc}} = \left(\left(\frac{\epsilon_s^2}{\epsilon_s^2 - \epsilon^2_{s\_metal}} \right) \sigma^2_{\epsilon_s} + \left(\frac{\epsilon^2_{s\_metal}}{\epsilon_s^2 - \epsilon^2_{s\_metal}} \right) \sigma^2_{\epsilon_{s\_metal}} \right)^{1/2} \tag{42}$$

4.1.2 Recommended Experimental Parameters

The sample calculations above demonstrate what realistic goals can be set to determine the screening energy of superconducting PdD. Based on the sample calculations, the following experimental parameters are recommended.

- 20 keV deuteron energy (to enable full use of these calculations)
- Establish x=~0.9 in PdD to ensure calculations match the physical conditions in the material
- Allow for 5% increase in PdD loading to establish an average T_c of 9-11 K
- Carry out experiment in shortest times possible to minimize the background counts while understanding cooling limitations and detector dead time
- Minimize temperature differential in PdD by having the sample not much larger than the penetration depth of deuterons
- Ensure sample thickness is greater than the coherence length PdD (~100 Å)[28] and penetration depth (1000 Å), which is more restrictive
- Prevent other charged fusion products from entering detector by adding shielding with low intrinsic activity

Chapter 5
Possible Engineering System

How is it possible to take advantage of fusion cross section enhancement for a possible energy extraction system? It is clear that without enhanced screening, the likelihood of fusion is so low that solid state fusion would not result in net gain fusion. If the Chapter 4 enhancement in superconductors is considerable it may be reasonable to consider engineering a system to extract the fusion energy.

The key parts required for a superconducting fusion system are the following:

- A material that enables enhanced fusion reactions
- A means of inducing the fusion reactions (e.g., external ion acceleration or internal vibration energy)
- A means of extracting the energy from the fusion products

Fig. 6 is an example system design to support the energy conversion of superconducting fusion. A superconductor rod or plate is in the center with a cooling channel through the center of it. Cooling would be required, because some fusion product energy would be deposited in the superconductor. The key to extracting energy from a system below room temperature is to use direct ion-to-electric conversion, a form of Direct Energy Conversion (DEC). A means of DEC can be represented by two metal spheres concentric with each other. The negative inner shell is ion permeable, and the positive outer shell is solid metal. As each charged particle passes through the grid it is slowed down and captured in the positive shell. This converts the kinetic energy into potential energy. However, fusion reaction energies can differ leading to wasted energy. To minimize variable fusion product energy loss, a more elaborate DEC system, like the "Venetian Blind" system from R. Moir could be used.[39]

5.1 Estimating Energy Gains

This section discusses a general analysis framework to estimate if a superconducting fusion systems can result in net energy gain. The gain calculation begins with the energy input required, E_i. This term includes cooling requirements and ion energy input. Next, fusion reactions will result in an energy output. For the DEC system discussed above, the output energy that can convert to electricity, E_o, can only be charged fusion products. Energy lost by the ions exiting the superconductor must be considered. The fusion reaction probability must also be defined by multiplying the integrated fusion cross section, σ_i, by the number density, N, of the material. The amount of energy that can be converted in the DEC system is limited by the conversion efficiency and the fraction of fusion ions that reach the DEC system. With R. Moir's work we can assume that the conversion efficiency is ~70%.[39] Assuming only a fraction of the fusion products energy will exit the surface, the DEC efficiency of those charged particles, or η, is 0.7. Combining these factors results in

$$G = N \cdot \sigma_i \cdot \frac{E_o}{E_i} \cdot \eta \tag{43}$$

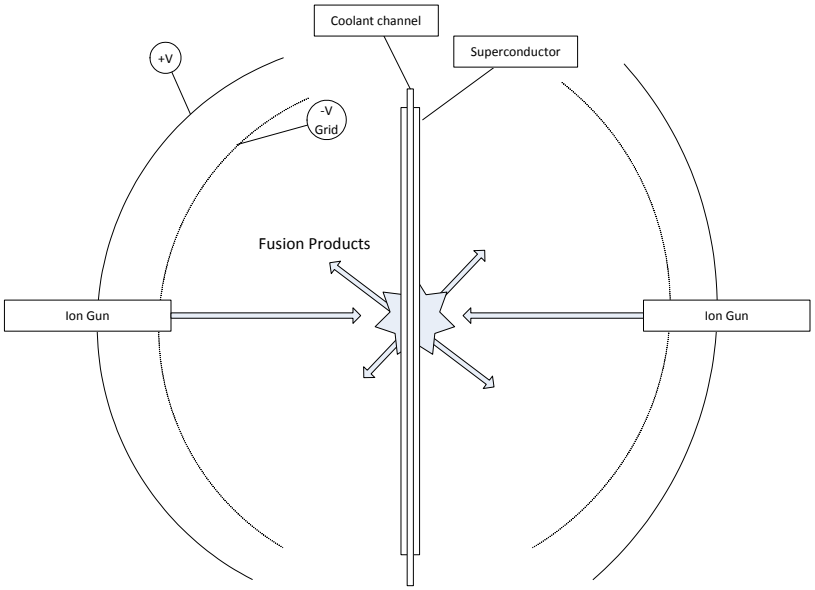

Figure 6. Possible Energy Extraction System

For a lattice vibration induced system, the gain equation is written without $N\sigma_i$. This is because no projected ions are used.

$$G = \frac{E_o}{E_i} \cdot \eta \tag{44}$$

The energy loss sources will be discussed next.

5.1.1 Energy Losses

With the possible engineering system using ion implantation methods, energy losses (i.e., heat) exist in the following forms:

- Ion implantation that does not result in fusion $\Longrightarrow E_{ion}\left(1 - N\sigma_i\right)$
- Fusion product energy deposition in superconductor $\Longrightarrow \overline{F_{Edep}} E_{fusion} N\sigma_i$
- Inefficiency in direct energy conversion $\Longrightarrow (1-\eta)\left(1 - \overline{F_{Edep}}\right) E_{fusion} N\sigma_i$

where E_{ion} is the incoming ion energy, $\overline{F_{Edep}}$ is the average fraction of energy deposited in the superconductor from charged fusion products, E_{fusion} is the charge particle energy released from fusion, and $(1-\eta)$ is the fraction of energy that is unable to be converted to electricity at the DEC location.

Putting these losses into equation form the following energy waste per implanted ion is

$$E_{waste} = E_{ion}\left(1 - N\sigma_i\right) + \overline{F_{Edep}} E_{fusion} N\sigma_i + (1-\eta)\left(1 - \overline{F_{Edep}}\right) E_{fusion} N\sigma_i \tag{45}$$

The cost of energy to remove the waste energy is

$$E_{cost\_1} = \frac{E_{waste}}{COP} \tag{46}$$

This is conservative in that it assumes that energy lost as heat at the DEC device will have to be removed at the same COP, or Coefficient of Performance, as the superconductor temperature. The COP of a cooling system indicates how many units of heat can be removed with one unit of work. More accurately, E_{cost} is defined as

$$E_{cost\_2} = \frac{E_{ion}\left(1 - N\sigma_i\right) + \overline{F_{Edep}} E_{fusion} N\sigma_i}{COP_1} + \frac{\left(1-\eta\right)\left(1 - \overline{F_{Edep}}\right) E_{fusion} N\sigma_i}{COP_2} \quad (47)$$

where COP_1 and COP_2 correspond to the COP of the superconductor's temperature and the DEC temperature respectively.

If a material is able to show that lattice vibrations are sufficient to cause fusion reactions with adequate energy density without incoming ions, then E_{waste} can be written as

$$E_{cost\_3} = \frac{\overline{F_{Edep}} E_{fusion}}{COP_1} + \frac{\left(1-\eta\right)\left(1 - \overline{F_{Edep}}\right) E_{fusion}}{COP_2} \quad (48)$$

An additional energy loss that does not contribute to heating the system is the energy loss to electrons that subsequently emit x-rays. To be conservative, lost x-ray radiation will be included in the heat removal requirement.

5.1.1.1 Fusion Energy Deposition

To find $\overline{F_{Edep}}$ one must consider the possible paths that the fusion products will take when exiting the material. These paths are shown in Fig. 7. If the angle (θ) is small enough, then the fusion charged particles will be trapped contributing to $\overline{F_{trapped}}$, or the average fraction of trapped fusion charged particles. Even if a charged particle is not trapped, some of the ion's energy will be deposited in the lattice nuclei and electrons through collisions. The amount of energy loss from the products will be related to the chosen sample thickness (t). Fusion product trajectories will be considered isotropic. For conservatism and ease, the angles will range from 0 - 90 degrees, and the source of fusion will be located at the bottom of the sample. Any ion emission angle that results in a distance traveled through the material that is greater than the projected range in the material the ion will be modeled as trapped in the material. Thinner samples will result in smaller maximum angles of fusion product trapping. At the limit of a superconductor thickness equal to ξ_o (~100 Å) the limiting penetration depth of a 0.82 MeV, He-3, D-D fusion product ($1.12 \times 10^{-6}\,\mathrm{m}$) results in maximum angle of trapping of $\arcsin\left(t/d\right) \approx 0.6°$. If the thickness were increased by ten times, the maximum angle of trapping ($\theta_{\max}$) would be ~5°. So this equates to a conservative $\overline{F_{trapped}} = 0.6/90 = 0.00\ 67$ for the thin sample or $\overline{F_{trapped}} = 5/90 = 0.056$ for the ten times thicker sample. For simplicity, $\overline{F_{trapped}}$ will be applied to all emitted ion products.

To determine the energy deposition through collisions that do not result in a stopped, charged fusion product, the average distance d must be calculated. $\overline{d}$ is calculated below (in radians).

$$\overline{d} = t\frac{\int_{\theta_{\max}}^{\pi/2} \frac{1}{\sin(\theta)} d\theta}{\pi/2 - \theta_{\max}} \quad (49)$$

where $\theta_{\max}$ is the maximum angle of trapping and $\int \frac{1}{\sin(\theta)} d\theta = -\ln\left|\csc\left(\theta\right) + \cot\left(\theta\right)\right| + c$. [40] For PdD $t = 10^{-8}\,\mathrm{m}$, $\overline{d} = 1.74t$ and for $t = 10^{-7}\,\mathrm{m}$, $\overline{d} = 2.29t$. With this information

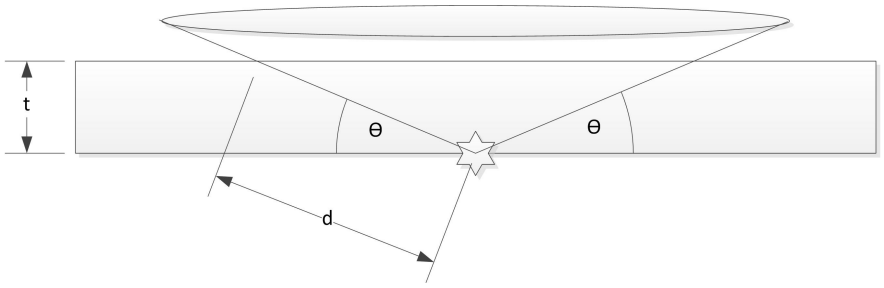

Figure 7. Exit Paths of Fusion Products

and the stopping power of each charge fusion product the $\overline{F_{Edep}}$ per D-D fusion event becomes (neglecting neutron heating)

$$\overline{F_{Edep}} = \frac{\left(\sum_{H-1,H-3,He-3} \overline{\frac{dE}{dx}_{ion}} \cdot \overline{d} \cdot \left(1 - \overline{F_{trapped}}\right) + \sum_{H-1,H-3,He-3} E_{ion} \cdot \overline{F_{trapped}}\right)}{\sum_{H-1,H-3,He-3} E_{ion}} \tag{50}$$

where E_{ion} is the initial energy of each fusion product and $\overline{\frac{dE}{dx}_{ion}}$ is the average stopping power of the fusion product from SRIM. $\sum_{H-1,H-3,He-3} E_{ion} = 4.85\,\mathrm{MeV}$. For D-D fusion in a PdD sample with $t = 10^{-7}\,\mathrm{m}$, the energy deposited is ~500 keV, and $\overline{F_{Edep}} \approx 0.1$. For $t = 10^{-8}\,\mathrm{m}$, the energy deposited is ~50 keV, and $\overline{F_{Edep}} \approx 0.01$.

With the established equations for energy losses, COPs will be discussed next.

5.1.1.2 Coefficient of Performances

Coefficient of Performances relate to how efficient heat can be removed from a possible fusion energy extraction system (e.g., superconductor). First, the theoretical cooling at Carnot efficiency will be considered. Second, an actual cooling device efficiency will be compared to the Carnot efficiency for perspective.

The Carnot efficiency of a refrigerant cycle is defined by a COP of [41]

$$COP = \frac{q_l}{w_{net,in}} = \frac{1}{T_H/T_L - 1} \tag{51}$$

where q_l is the heat removed, $w_{net,in}$ is the work energy required to remove that heat energy, T_H is the temperature of the area where the heat is rejected to, T_L is the desired temperature of the item to be cooled. If it is assumed that T_H is room temperature (~293K) the COP as a function of T_L is shown in Fig. 8.

Comparing the theoretical cooling COPs to an commercial systems from Sumitomo Cryogenics, the actual system cooling is less efficient as expected.

To improve the COPs, heat could be rejected to other locations besides typical room temperature. Heat could be rejected to the ground if it were a cooler location (i.e., lower T_H).

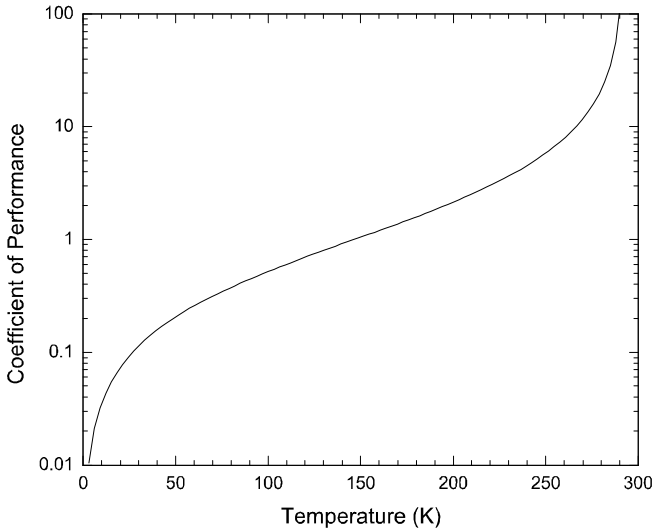

Figure 8. Coefficient of Performance with Heat Ejection to 293K Sink

Table 7. COPs of Commercial Cooling Devices

	Actual COP	Ideal COP Eq. 51
4.2 K [42]	$0.1\,\mathrm{W}/1.3\,\mathrm{kW} = 8 \times 10^{-5}$	$\frac{1}{293/4.2-1} = 0.015$
77 K [43]	$120\,\mathrm{W}/7.65\,\mathrm{kW} = 0.016$	$\frac{1}{293/77-1} = 0.36$

5.1.2 Sample Superconducting PdD Calculation

For D-D fusion events taking place in PdD, a sample gain calculation will considered based on Eq. 44 and Eq. 48. If superconducting PdD demonstrates high enough screening and, hence, enough fusion reactions at temperatures below T_c, then further investigating energy extraction is warranted. Of course, T_c may be greater than 11 K when loading is greater than x=1 according to Tripodi.

Assumptions in this calculation are:

(1) PdD sample $t = 10^{-8}m$
(2) For a reasonable Cooper pair density fraction as shown in Table 3, the superconductor temperature will be kept at $T_c/2$
(3) Carnot COPs will be used for calculation ease, while understanding that available system COPs at lower temperature are worse
(4) The DEC system will be arbitrarily kept at 5 K below room temperature
(5) Density of fusion events and radiation destruction of the superconducting state are not

considered

Rewriting Eq. 44 specifically for this sample calculation

$$G = \frac{\left(\sum_{H-1,H-3,He-3} E_{ion}\right)\left(1 - \overline{F_{Edep}}\right)}{E_{cost\_3}} \cdot \eta \tag{52}$$

where $\sum_{H-1,H-3,He-3} E_{ion} = 4.85\,\mathrm{MeV}$, $\overline{F_{Edep}} \approx 0.01$, $\eta = 0.7$ and E_{cost_3} from Eq. 48 with appropriate values filled in

$$E_{cost\_3} = \frac{0.01 \cdot 4.85\,\mathrm{MeV}}{\left(293K/\left(T_c/2\right) - 1\right)^{-1}} + \frac{\left(1 - 0.7\right)\left(1 - 0.01\right)4.85\,\mathrm{MeV}}{\left(293K/\left(287K\right) - 1\right)^{-1}} \tag{53}$$

and the gain becomes

$$G = \frac{3.36}{0.485\left(293/\left(T_c/2\right) - 1\right) + 0.030} \tag{54}$$

This hypothetical energy gain versus critical temperature is shown in Fig. 9. This calculation only utilizes Carnot efficiency and does not address the higher stopping power that would exist with higher loaded PdD with x>1 that may enable higher transition temperatures discussed in Section 2.1.2. This is the energy gain from one fusion event that can be emitted out of either side of PdD plate toward a DEC. It is clear that the energy gain from a PdD sample, with the widely accepted $T_c = 11\,\mathrm{K}$, is less than one. These calculations do not take into account the thermal conductivity and heat capacity of the superconductor that could restrict heat transfer for cooling.

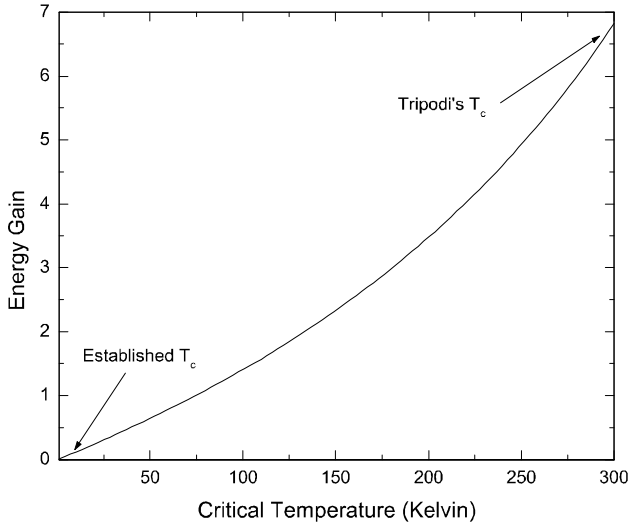

Figure 9. Hypothetical Energy Gain Versus Critical Temperature of PdD

Chapter 6
Conclusion

The feasibility of a D-D fusion experiment in superconducting PdD has been demonstrated, revealing an expected 38% error of the screening energy with 95% confidence. This would help provide closure on the long debate on the effect of Cooper pair screening on charges. If the superconductor screening effect is significantly greater than ion screening in metals, then two additional experiments are warranted. First, determine the screening effect with superconducting atoms that have inner orbital electrons (i.e., MgB_2). Second, if deuterium is not a base element in a high temperature superconductor, determine if D-D fusion reactions exhibit superconductor screening. This second experiment may have implications when considering a fusion energy system.

This research has also established that no net energy gain would result from superconducting fusion with T_c below 100 K. Therefore, fusion in superconducting PdD at the accepted T_c of 11 K would not result in net energy gain. Even if PdD_x, with $x \gg 1$, were a high temperature superconducting as Tripodi proposes, the fusion reaction rate from lattice vibrations appear to be insufficient to support auxiliary systems (e.g., vacuum pump). The only way to overcome the energy losses of cooling and auxiliary systems would be to drastically increase the fusion reaction rate (e.g., increase the deuteron number density or nearest neighbor density, or decrease the lattice spacing) in a high temperature superconductor. Of course, new net gain calculations would have to be completed to validate how a specific material would perform.

References

[1] Krane, K. Modern Physics, Second Edition. (Wiley: 1996).

[2] Atzeni, S. & Meyer-Ter-Vehn, J. The physics of inertial fusion. (Oxford University Press: 2004).

[3] Dolan, T. Fusion Research. (2000).

[4] Liolios, T.E. The role of electron-screening deformations in solar nuclear fusion reactions and the solar neutrino puzzle. Nuclear Physics A 683, 713-726(2001).

[5] Trautvetter, H. Charged-particle thermonuclear reactions. Journal of Physics G: Nuclear and Particle 19, S95-S102(1993).

[6] Huke, A. et al. Enhancement of deuteron-fusion reactions in metals and experimental implications. Physical Review C 78, 15803(2008).

[7] Shibata, K. & Kodama, R. Significant reduction of the internuclear potential in superconductive solid metallic hydrogen. Journal of Physics: Condensed Matter 20, 075231(2008).

[8] Raiola, F. et al. Electron Screening: A Review. Frontiers in Nuclear Structure, Astrophysics, and Reactions 831, 296–303(2006).

[9] Rolfs, C. Electron screening in metallic environments: a plasma of the poor man. Origin of Matter and Evolution of Galaxies(AIP Conference Proceedings) 847, 245–248(2006).

[10] Kittel, C. Introduction to Solid State Physics. (Wiley: NY, 1996).

[11] Dressel, M. & Gruner, G. Electrodynamics of solids. (Cambridge University Press Cambridge: UK, 2003).

[12] Nave, R. Hyperphysics. (Georgia State University: GA, 2010). <http://hyperphysics.phy-astr.gsu.edu/hbase/hframe.html>

[13] Fujita, S. & Godoy, S. Quantum Statistical Theory Of Superconductivity (Springer: NY, 1996).

[14] Lipavsky, P. et al. Bernoulli Potential in Superconductors. (Springer: 2008).

[15] Koyama, T. Comment on “Charge expulsion and electric field in superconductors”. Phys. Rev. B 70, 226503(2004).

[16] Hirsch, J. Reply to “Comment on ‘Charge expulsion and electric field in superconductors’ ”. Phys. Rev. B 70, 226504(2004).

[17] Stoppini, G. Coulomb screening in superconducting PdH. Il Nuovo Cimento D 13, 1181–1188(1991).

[18] Oliveira Santos, F. Nuclear astrophysics with light nuclei at GANIL. Frontiers in Nuclear Structure, Astrophysics, and Reactions(2010).

[19] Bonomo, C. Enhanced electron screening in d (d, p) t for deuterated metals. The European Physical 719, C37-C42(2003).

[20] C. Angulo, et al., A Compilation of Charged-Particle Induced Thermonuclear Reaction Rates. Nucl. Phys. A656(1999)3-187. <http://pntpm3.ulb.ac.be/Nacre/barre_database.htm>

[21] Steiner, D. Introduction to Fusion Devices and Systems. (RPI: NY, 2005).

[22] Fukai, Y. The Metal-Hydrogen System, Second Edition. (Springer: 2005).

[23] Tripodi, P., Di Gioacchino, D. & Vinko, J.D. Magnetic and transport properties of PdH:

intriguing superconductive observations. Brazilian Journal of Physics 34, 1-8(2004).

[24] Tripodi, P. High T_c Palladium Hydride Superconductor. US Patent 7,033,568(2006).

[25] Baranowski, B. & Debowska, L. Remarks on superconductivity in PdH. Journal of Alloys and Compounds 437, L4-L5(2007).

[26] Tripodi, P., Di Gioacchino, D. & Vinko, J.D. Answer to the remarks on superconductivity in PdH. Journal of Alloys and Compounds 470, L6-L8(2009).

[27] Vaidya, S. On the Possibility of Nonequilibrium High-Temperature Superconductivity in PdH and PdD (*). Il Nuovo Cimento D 13, 1449-1451(1991).

[28] Heim, G. & Stritzker, B. Ion Implantation A Powerful Technique for the Production of Metastable Superconducting Alloys. Appl. Phys.7, 239 248(1975).

[29] Ziegler, J. & Biersack, J. SRIM - Stopping and Range of Ions in Matter. 2008.04 Code, IBM Company.

[30] Canfield, P. & Crabtree, G. Magnesium Diboride: Better Late than Never. Physics Today (2003).

[31] Geuther, J. Radiation Generation with Pyroelectric Crystals. Doctoral Thesis. (RPI: NY, 2007).

[32] Fiorentini, G. et al. Fusion rate enhancement due to energy spread of colliding nuclei. Physical Review C 67, 14603(2003).

[33] Hsu, D. & Leisure, R. Elastic constants of palladium and the β-phased palladium hydride between 4 and 300 K. Phys. Rev. B 20, 4(1979).

[34] Ichimaru, S. Nuclear fusion in dense plasmas. Reviews of Modern Physics 65, 255(1993).

[35] Chambers, G., Eridon, J., & Grabowski, K. Upper limit on cold fusion in thin palladium films. Phys. Rev. B 41, 8(1990).

[36] Knoll, G. Radiation Detection and Mesurement, Third Edition. (Wiley: 2000).

[37] Kasagi, J. Screening Potential for Nuclear Reactions in Condensed Matter. ICCF-14 1-7(2008).

[38] Greife, U., et al. Oppenheimer-Phillips effect and electron screening in d+ d fusion reactions. Z. Phys. A 351, 107-112(1995).

[39] Moir, R. & Barr, W. "Venetian Blind" Direct Energy Conversion for Fusion Reactors. Nuclear Fusion 13(1973).

[40] Larson, R., Hostetler, R., & Edwards, B. Calculus: Early Transcendental Functions, Third Edition. (Houghton Mifflin: 2003).

[41] Cengel, Y. & Boles, M. Thermodynamics An Engineering Approach. (McGraw-Hill: 2005).

[42] Sumitomo Cryogenics Group. Model SRDK-101D-A11C. (2011).

[43] Sumitomo Cryogenics Group. Model CH-210. (2011).